Analyst

RSC Publishing

PAPER

View Article Online
View Journal

Cite this: DOI: 10.1039/c3an01587d

A highly sensitive electrochemical aptasensor for thrombin detection using functionalized mesoporous silica@multiwalled carbon nanotubes as signal tags and DNAzyme signal amplification†

Juan Zhang, Yaqin Chai,* Ruo Yuan,* Yali Yuan, Lijuan Bai and Shunbi Xie

In this work, we demonstrated a novel sensitive sandwich-type pseudobienzyme aptasensor for thrombin detection. Greatly amplified sensitivity was based on mesoporous silica-multiwalled carbon nanotube ($mSiO_2$@MWCNT) nanocomposites as enhanced materials and a pseudobienzyme electrocatalytic system. Firstly, the $mSiO_2$@MWCNT nanocomposites not only have good biocompatibility and a suitable microenvironment for stabilizing the aptamer assembly, but also can load large amounts of electron mediator thionine (Thi), platinum nanoparticles (PtNPs) and hemin/G-quadruplex bioelectrocatalytic complex. Moreover, in the presence of H_2O_2 in an electrolytic cell, the synergistic reaction of PtNPs and hemin/G-quadruplex bioelectrocatalyzed the reduction of H_2O_2, dramatically amplifying the response signals of electron mediator Thi and improving the sensitivity. Secondly, dendrimer functionalized reduced graphene oxide (PAMAM–rGO) as the biosensor platform enhanced the surface area for the immobilization of abundant primary aptamers as well as facilitated electron transfer from Thi to the electrode, thus amplifying the detection response. Using the above multiple effects, the approach showed a high sensitivity and a wider linearity for the detection of thrombin in the range between 0.0001 nM and 80 nM with a detection limit of 50 fM. This new design avoided the fussy labeling process and the spatial distribution of each sequentially acting enzyme, which provided an ideal candidate for the development of a sensitive and simple bioanalytical platform.

Received 21st August 2013
Accepted 7th September 2013

DOI: 10.1039/c3an01587d

www.rsc.org/analyst

Introduction

Rapid and sensitive assays for the quantitative detection of biomarkers composed of proteins or nucleic acids are critical to many areas, for example, clinical diagnosis, biomedical research, and biodefense application.[1–3] At present, extensive efforts have been devoted to the development of aptamer-based sensors including fluorescent sensors,[4] colorimetric sensors,[5] luminescent sensors,[6] electrochemical sensors,[7] quartz crystal microbalance sensors,[8] and surface plasmon resonance sensors.[9] Among them, electrochemical aptasensors, due to their distinct advantages of intrinsic simplicity, high specificity, fast response, low production cost and relative miniaturization, have received particular attention in recent years. To date, aptamer-based signal amplification platforms, such as nanomaterials,[10,11] nanoparticles[12] and enzymes,[13] have been rapidly developed to detect different targets by combining various electrochemical techniques with aptasensor signal conversion strategies.

Recently, in aptasensor design,[14,15] there has been an explosion of interest in nanomaterial synthesis and their application in the area of bioassays.[16] Among all different kinds of nanomaterials, carbon nanotubes (CNTs) have inspired a vast range of promising applications due to the high surface area, excellent electronic conductivity, and high chemical stability.[17–19] Wildgoose *et al.* reviewed the recent developments in this area by exploring the various techniques to functionalize CNTs with metals and other nanoparticles.[20] However, the application of CNTs has been impeded by their poor solubility in solvents and polymers, which originates from strong van der Waals attraction among CNTs. Without surface modification, most CNTs have poor dispersion and aggregation of metal nanoparticles, especially under high loading conditions. Therefore, functionalization of CNTs is generally prerequisite for further applications.[21–23] Recently SiO_2, an inorganic cross-linked shell, has been the most widely studied owing to its superior advantages such as a high specific surface area, biocompatibility and a highly porous structure.[24] The formation of a SiO_2 shell on the surface of CNTs will not only effectively improve the solubility of CNTs to a certain extent, but also provide a high surface area

Education Ministry Key Laboratory on Luminescence and Real-Time Analysis, College of Chemistry and Chemical Engineering, Southwest University, Chongqing 400715, People's Republic of China. E-mail: yuanruo@swu.edu.cn; yqchai@swu.edu.cn; Fax: +86-23-68253172; Tel: +86-23-68252277

† Electronic supplementary information (ESI) available. See DOI: 10.1039/c3an01587d

with a porous structure,[25] leading to a satisfactory biomaterial for constructing high-sensitivity electrochemical aptasensors. In addition, biocompatible reduced graphene oxide (rGO) as a sensor platform has several advantages for the design of aptamer-based electrochemical analytical devices. Firstly, it presents an abundant domain for biomolecular binding. Secondly, it also speeds up electron transfer from an electron mediator and further amplifies the electrochemical signal.[26] Carboxyl-terminated polyamidoamine (PAMAM G4.5), hyperbranched and three-dimensional with adequate functional groups, can also be used to modify the electrode surface for chemical fixation.[27] Therefore, in this work, we construct an electrochemical aptasensor with PAMAM–rGO as the biosensor platform for amplification of the detection response.

Functional nucleic acids (FNA),[28] including DNA aptamers[29] (single-stranded DNA molecules that can specifically bind to a non-nucleic acid target) and DNA enzymes[30] (DNAzymes) (DNA molecules that are capable of catalyzing chemical reactions) represent an emerging class of biomolecules having great advantages in bioassay development. DNAzymes are of growing interest as amplifying labels to amplify biosensing events. Recently, the horseradish peroxidase-mimicking DNAzyme (HRP-mimicking DNAzyme) that consists of hemin intercalated in a G-quadruplex structure has attracted special attention and is probably the most frequently used biocatalytic DNAzyme label.[31] For example, a variety of optical or chemiluminescence enzyme-based biosensors, DNA sensors, or aptasensors using the HRP-mimicking DNAzyme as an amplifying label are reported.[32–34] In these reports, DNAzymes are used to catalyze the oxidation of 2,2-azino-bis(3-ethylbenzothiazoline-6-sulfonic acid) (ABTS) to produce the colored radical ion ($ABTS^{-}$) or generate chemiluminescence through the oxidation of luminal by H_2O_2, and simultaneously show great catalytic activity toward H_2O_2.[35] It is known that the thrombin binding aptamer (TBA) possesses a G-quadruplex that could be intercalated by hemin to form a hemin/G-quadruplex structure, showing higher electrocatalytic ability compared to free hemin.[36]

In this contribution, a novel sensitive sandwich-type pseudobienzyme aptasensor was developed for thrombin assay based on mesoporous silica-multiwalled carbon nanotube ($mSiO_2$@MWCNT) nanocomposites as magnified materials and hemin/G-quadruplex as a HRP-mimicking DNAzyme for signal enhancement. In this aptasensor, the PAMAM–rGO nanohybrid composed of rGO and PAMAM as the biosensor platform was first self-assembled on a glassy carbon electrode (GCE), which provided a large accessible surface area to capture a large number of primary aptamers and also facilitated electron transfer from the electron mediator thionine (Thi) to the electrode for amplifying the detection response. Additionally, mesoporous silica was functionalized on the surface of multiwalled carbon nanotubes. The superior $mSiO_2$@MWCNT nanocomposites not only had good biocompatibility and a suitable microenvironment for stabilizing the aptamer assembly, but also provided an effective platform for anchoring large amounts of electron mediator Thi, platinum nanoparticles (PtNPs) and hemin/G-quadruplex bioelectrocatalytic complex with high stability and bioactivity. Subsequently, the hemin/G-quadruplex was formed by intercalating hemin into the thrombin binding aptamer (TBA). Through sandwich reactions, the hemin/G-quadruplex conjugated PtNP–Thi–$mSiO_2$@MWCNT nanocomposites were captured on a PAMAM–rGO nanohybrid modified electrode surface. In the presence of H_2O_2 in an electrolytic cell, PtNPs and the hemin/G-quadruplex as a HRP-mimicking DNAzyme on the electrode surface bioelectrocatalyzed the reduction of H_2O_2, which dramatically improved the oxidation–reduction reaction of electron mediator Thi and resulted in an obvious amplification in the electrochemical signal. Finally, according to the linearity between TB concentration and current response, we could sensitively detect thrombin with a low detection limit. This work provided a promising way for broad potential application in clinical assays and various protein analyses.

Experimental

Chemicals and materials

Thrombin (TB), hemin, thionine (Thi), hemoglobin (Hb), bovine serum albumin (BSA), polyethyleneimine (PEI), hexadecyltrimethylammoniumbromide (CTAB, 99%), carboxyl-terminated polyamidoamine (G4.5 PAMAM), and chloroplatinic acid (H_2PtCl_6) were purchased from Sigma-Aldrich Chemical Co. (USA). Graphene oxide (GO) and multiwalled carbon nanotubes (MWCNTs) were obtained from Nanjing xianfeng nano Co. (China). *N*-Hydroxy succinimide (NHS) and 1-ethyl-3-(3-dimethylaminopropyl) carbodiimide hydrochloride (EDC) were acquired from Shanghai Medpep Co. (China). $NaBH_4$ was obtained from Kelong Chemical Company (Chengdu, China). Thrombin binding aptamer (TBA): 5′-NH_2-$(CH_2)_6$-GGTTGGTGTGGTTGG-3′ TBA was purchased from TaKaRa (China). Trishydroxymethylaminomethane hydrochloride (Tris–HCl) was supplied by Roche (Switzerland). A 0.1 M phosphate buffered solution (PBS, pH 7.0) containing 10 mM Na_2HPO_4, 10 mM KH_2PO_4 and 2 mM $MgCl_2$ was used as a working buffer. 20 mM Tris–HCl buffer (pH 7.4) containing 100 mM NaCl was used as a binding buffer. All other chemicals were of reagent grade and used as received.

Apparatus

Cyclic voltammetry (CV) and differential pulse voltammetry (DPV) measurements were carried out on a CHI 610A electrochemical workstation (Shanghai Chenhua Instrument, China). pH measurements were made with a pH meter (MP 230, Mettler-Toledo, Switzerland). All experiments were performed in a conventional three-electrode system: a platinum wire auxiliary electrode, a saturated calomel reference electrode (SCE) and a modified glassy carbon electrode (GCE, $\Phi = 4$ mm) as the working electrode. Scanning electron micrographs were taken with a scanning electron microscope (SEM, S-4800, Hitachi, Japan). Transmission electron micrograph (TEM) images were recorded on a JEOL-JEM 2100 transmission electron microscope (Oxford Instrument, Japan).

Preparation of PAMAM–rGO

Firstly, reduced graphene oxide sheets (rGO) were prepared according to the literature with a little modification.[26] Briefly, a

3% PEI (1 mL) solution used as reductant was added to a 0.5 mg mL^{-1} exfoliated GO dispersion (30 mL), and it was then heated under reflux at 135 °C for about 3 h. The obtained black rGO dispersion was subjected to centrifugation at 10 000 rpm for 15 min and washed several times with double distilled water. Then, PAMAM functionalized rGO (PAMAM–rGO) was synthesized by conjugating rGO (l mg mL^{-1}, 2 mL) and PAMAM (1 mg) with EDC and NHS acting as coupling agents. As shown in Fig. 1A, the SEM image of dendrimer functionalized reduced graphene oxide showed a homogeneous coverage of PAMAM and good dispersion, which presented a large specific surface area and good biocompatibility for the immobilization of aptamers.

Coating mesoporous SiO_2 on MWCNTs ($mSiO_2$@MWCNTs)

Prior to experiments, a simple procedure to coat a porous SiO_2 layer on multiwalled carbon nanotubes (MWCNTs) with the aid of the cationic surfactant cetyltrimethyl ammonium bromide (CTAB) was performed according to a previously reported method with slight modifications.[25] In a typical synthesis, MWCNTs, CTAB and H_2O were mixed in the ratio of 1 mg/10 mg/1 mL, and ultrasonically dispersed for 3 hours to form a stable dispersion. 0.5 mL of the as-prepared MWCNT dispersion, 4 mL of H_2O and 0.5 mL of NaOH aqueous solution (0.01 M) were added into a vial in sequence and ultrasonically treated for 1 min, and then the vial was heated to 60 °C. 20 minutes later, 25 μL of a tetraethylorthosilicate (TEOS)–ethanol (v/v = 1/4) solution was injected into the vial. After shaking mildly for 30 seconds, this vial was heated at 60 °C without stirring for 12 hours. After the coating process, the product was washed at least 5 times by centrifugation and redispersion in ethanol to remove the surfactant thoroughly, and dried for 4 h at 60 °C. Fig. 1B shows TEM images of the as-prepared $mSiO_2$@MWCNT nanocomposites. Compared with the TEM image of MWCNTs (Fig. 1C), it is seen that there are some high-quality nanosheets with a rough surface and many nanopores in individual nanosheets, indicating the feasibility of our method. In further analysis of the chemical composition of the MWCNTs and $mSiO_2$@MWCNT nanocomposites, SEM images (Fig. 1D and E) provided further evidence for the successful preparation of $mSiO_2$@MWCNT nanocomposites.

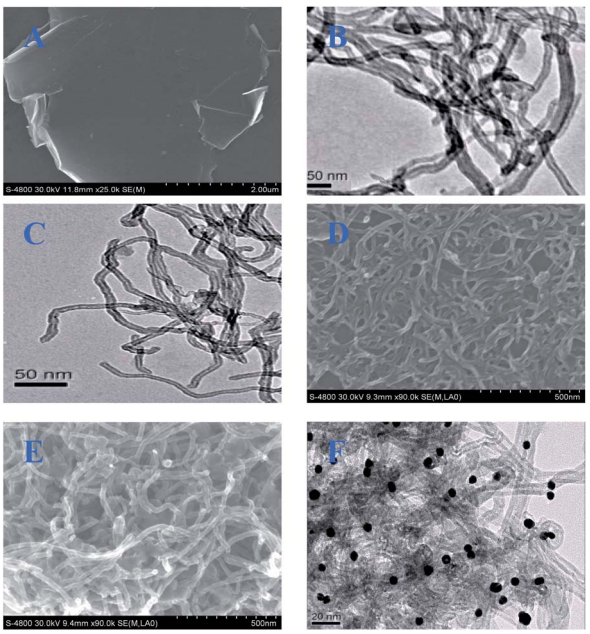

Fig. 1 SEM image of PAMAM–rGO (A), TEM images of $mSiO_2$@MWCNTs (B) and MWCNTs (C), SEM images of MWCNTs (D) and $mSiO_2$@MWCNTs (E) and TEM image of $mSiO_2$@MWNTs–Thi–PtNPs (F).

Preparation and bioconjugation of PtNP–Thi decorated $mSiO_2$@MWCNT composites

$mSiO_2$@MWCNT composites were decorated with thionine and platinum nanoparticles (PtNPs) as follows: 5 mg of $mSiO_2$@MWCNT composites were initially dispersed into 2 mL of distilled water, and 500 μL of Thi (3 mM) aqueous solution was then added into the as-prepared dispersion. Afterwards, the mixture was adequately stirred for 24 h at room temperature to make the positively charged thionine molecules adsorb onto the surface of negatively charged $mSiO_2$@MWCNTs. The obtained mixture was collected by centrifugation and was redispersed into 2 mL of distilled water. 4 mL of H_2PtCl_6 (1%, w/w) was injected into the mixture and incubated for 10 h at room temperature with slight stirring to make the negatively charged $PtCl_6^{2-}$ ions adsorb onto the Thi–$mSiO_2$@MWCNT composite surface. Then, 10 mL $NaBH_4$ (0.1 M) solution was added dropwise into the mixture with stirring for 30 min, followed by centrifugation, and dispersed into 2 mL of Tris–HCl buffer solution, pH 7.4, for further bioconjugation of the thrombin aptamer. When PtNPs were reduced onto Thi–$mSiO_2$@MWCNTs, the TEM image (Fig. 1F) showed some uniformly distributed PtNPs on the surface of the Thi–$mSiO_2$@MWCNT composites. It was important for effectively magnifying the loading amounts of TBA, thus leading to the high-sensitivity sensors.

Preparation of hemin/G-quadruplex conjugated $mSiO_2$@MWCNTs–Thi–PtNPs (secondary aptamer)

It is reported that PtNPs have strong adsorption ability for thiol and amino groups.[37,38] Thus, the hemin/G-quadruplex conjugated $mSiO_2$@MWCNTs–Thi–PtNPs were synthesized (Scheme 1A) according to the following steps. Firstly, 2 mL of the above $mSiO_2$@MWCNT–Thi–PtNP suspension was mixed with 0.1 mL amino TBA (2 μM) and incubated at 4 °C for 12 h under gentle stirring. Subsequently, 0.5 mg hemin was added into the above solution with an extra reaction time of 2 h. Then, BSA (1%) was put into the solution to block the unmodified portion of the $mSiO_2$@MWCNT–Thi–PtNP surface with a reaction time of 45 min. After centrifugation and washing, the final bioconjugate was resuspended in 2 mL Tris–HCl buffer and stored at 4 °C for further use. For the comparison of performance based on different labeled probes, a series of control experiments with different types of labeled probes synthesized in a similar way were carried out in order to

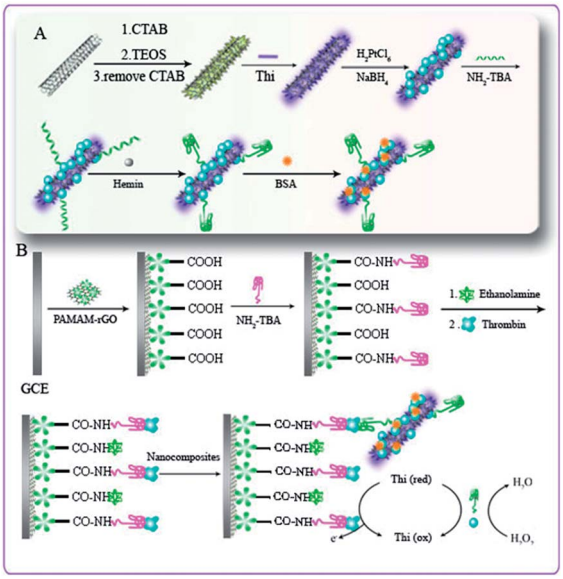

Scheme 1 Illustration of the electrochemical aptasensor based on PAMAM–rGO as a platform, functionalized $mSiO_2$@MWCNTs as signal tags and hemin/G-quadruplex as a HRP-mimicking DNAzyme for signal amplification.

demonstrate the substantial amplification capability of the proposed new protein detection strategy.

Fabrication of the modified electrodes

The sensing protocol for one-spot signal-on detection of thrombin is shown in Scheme 1B. Prior to use, a bare glassy carbon electrode (GCE) was carefully polished to a mirror-like surface with 1.0 and 0.3 μm alumina powder and sonicated sequentially in water, ethanol and water for a few minutes. Subsequently, 6 μL of the PAMAM–rGO solution was self-assembled onto the pretreated GCE to increase the effective area of the electrode, and the electrode was dried at room temperature. Then 20 μL of EDC (20 mM) and NHS (40 mM) solution was coated on the electrode to activate the carboxyl terminal of PAMAM for 2 h. After washing with double distilled water to remove the remains on the surface, the modified electrode was incubated with amino-terminated primary TBA (2 μM) for 1 h at room temperature. Finally, ethanolamine as a blocking reagent was added dropwise and the electrode was incubated for 1 h to eliminate nonspecific binding effects and block the remaining active groups. The finished aptasensor was stored at 4 °C for further use.

The detection of TB was based on the typical process for a sandwiched assay. Firstly, the aptasensor was incubated with 20 μL of thrombin standard solutions of different concentrations for 40 min at room temperature, followed by washing. Then, the electrode was also subjected to a water washing process, which was followed by incubation of 20 μL of the as-prepared hemin/G-quadruplex conjugated $mSiO_2$@MWCNTs–Thi–PtNPs for 40 min. After rinsing thoroughly with PBS to remove the unbound bioconjugate, the electrochemical detection was carried out in an electrolytic cell containing 2 mL 0.1 M PBS (pH 7.0) and 2.0 mM H_2O_2.

Electrochemical measurements

All electrochemical experiments were carried out in a conventional electrochemical cell, in which a modified working electrode, a SCE reference electrode and a Pt counter electrode were used. CV measurements were taken from −0.6 to 0.2 V (*vs.* SCE) at a scan rate of 100 mV s^{-1} in 2 mL 0.1 M PBS (pH 7.0). DPV measurements were performed in 2 mL 0.1 M PBS (pH 7.0) containing an appropriate amount of H_2O_2 to measure the performance of the aptasensor. The parameters applied were: 50 mV pulse amplitude, 50 ms pulse width, 0.2 s pulse period and voltage range from −0.6 to 0.2 V (*vs.* SCE).

Results and discussion

Electrochemical characterization of electrodes

The electrochemical characteristics and amplification performance of the aptasensor were investigated by CV measurements in 0.1 M PBS (pH 7.0). As seen in Fig. 2A, curves a and b show the CV waves of bare GCE and thrombin/ethanolamine/TBA/PAMAM–rGO modified electrodes, respectively. Because of the lack of substance with electrochemical activity in the working potential range, no peak was exhibited. When the $mSiO_2$@MWCNT–Thi–PtNP–hemin/G-quadruplex bioconjugate was assembled on the electrode surface *via* a sandwich-type assay, a stable and well-defined redox peak (Fig. 2A, curve c) was observed, indicating the excellent electron transfer and efficient redox activity of the bioconjugate. To demonstrate the dramatically amplified electrochemical signal induced by "sandwich" reactions, an appropriate amount of H_2O_2 was added into the solution. It could be easily seen that the cathodic peak current increased with the addition of H_2O_2 (Fig. 2A, curve d), indicating a typical electrocatalytic reduction process of

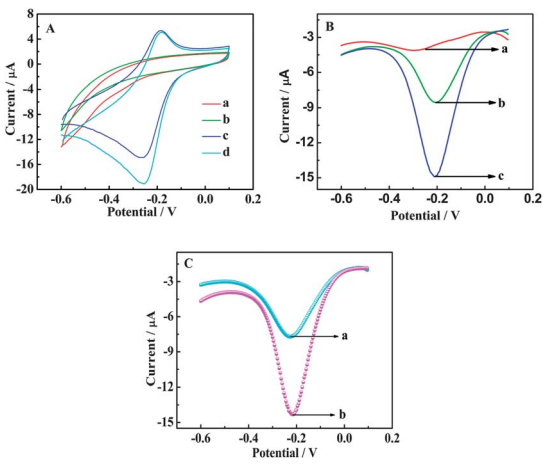

Fig. 2 (A) CVs of different modified electrodes in 0.1 M PBS (pH 7.0): (a) the bare GCE, (b) TB/ethanolamine/TBA/PAMAM–rGO/GCE, (c) after the sandwich format reaction of the resulting aptasensor in the absence and (d) in the presence of 2.0 mM H_2O_2 in the electrolytic cell. (B) DPVs obtained at (a) TB/ethanolamine/TBA/PAMAM–rGO/GCE and after the sandwich format reaction of the resulting aptasensor in the absence (b) and in the presence (c) of 2.0 mM H_2O_2 in the electrolytic cell. (C) DPVs of secondary aptamer/TB/ethanolamine/TBA/PAMAM/GCE (a) and secondary aptamer/TB/ethanolamine/TBA/PAMAM–rGO/GCE (b) in 0.1 M PBS (pH 7.0) containing 2.0 mM H_2O_2.

H_2O_2. Also, a sensitive electrochemical technique, DPV, had been used to obtain the direct electrochemical signal. After the aptasensor reacted with thrombin, the electrode was subjected to measurement in an electrolytic cell containing 2 mL 0.1 M PBS and 2.0 mM H_2O_2 and no obvious peak was seen (Fig. 2B, curve a). However, a dramatic electrochemical signal could be obtained when the secondary aptamer with the enhancement of the $mSiO_2$@MWCNT bioconjugate and a hemin/G-quadruplex pseudobienzyme bioelectrocatalytic structure reacted with thrombin in a sandwich-type assay in 2 mL 0.1 M PBS (pH 7.0) in the presence (Fig. 2B, curve c) and absence (Fig. 2B, curve b) of 2.0 mM H_2O_2, effectively providing the feasibility of a "sandwich" strategy. In addition, as shown in Fig. 2C, the proposed aptasensor (Fig. 2C, curve b) had a much higher current response than that without rGO as a sensor platform (Fig. 2C, curve a), indicating that rGO provided electron transfer tunnels and could facilitate the electron transfer between Thi and electrode.

Amplification properties of different conjugates

Taking advantage of the $mSiO_2$@MWCNT bioconjugate and the hemin/G-quadruplex pseudobienzyme bioelectrocatalytic structure as dual amplifications, amplification properties of the as-synthesized novel labels were investigated in different working buffers. Several types of labeled probes were used, such as Thi–PtNPs–hemin/G-quadruplex, MWCNTs–Thi–PtNPs–hemin/G-quadruplex and $mSiO_2$@MWCNTs–Thi–PtNPs–hemin/G-quadruplex. Fig. 3A and B show a low reduction peak current with inefficient bioelectrocatalysis of Thi–PtNPs–hemin/G-quadruplex and MWCNTs–Thi–PtNPs–hemin/G-quadruplex. As shown in Fig. 3C, the aptasensor with hemin/G-quadruplex conjugated $mSiO_2$@MWCNTs–Thi–PtNPs showed much greater electrochemical changes than those obtained *via* other methods, indicating the remarkable amplifying performance of this proposed label. This phenomenon may be attributed to the following reasons: $mSiO_2$@MWCNT nanocomposites not only have good biocompatibility but also increased surface area which can largely enhance the amount of Thi and PtNP assembly for signal amplification.

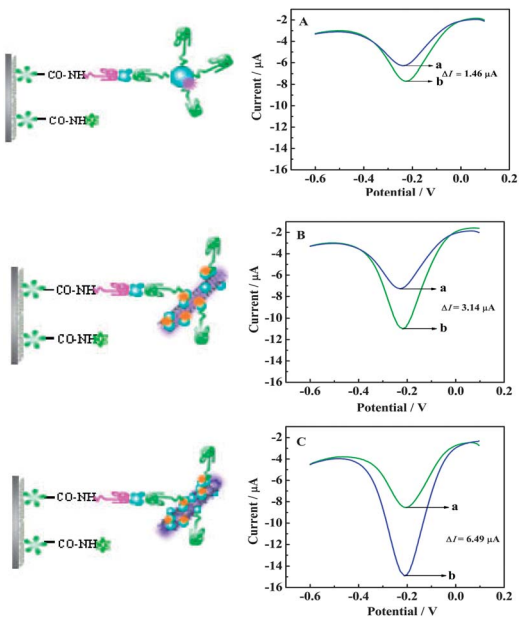

Fig. 3 The DPVs of the different sandwich format aptasensors in the absence (a) and in the presence (b) of 2.0 mM H_2O_2 in 0.1 M PBS (pH 7.0) obtained by using various labels: (A) Thi–PtNP–TBA–hemin/G-quadruplex labeled probe, (B) MWNT–Thi–PtNP–hemin/G-quadruplex labeled probe and (C) $mSiO_2$@MWNT–Thi–PtNP–hemin/G-quadruplex labeled probe.

The electroactive surface area of the PAMAM–rGO modified electrode

In order to illustrate that the prepared PAMAM–rGO nanohybrid film could improve the surface area and conductivity of the aptasensor, the electrochemical behaviors of different modified electrodes in 5.0 mM $Fe(CN)_6^{4-/3-}$ solution containing 0.1 M KCl at different sweep rates (υ) were investigated with the cyclic voltammetric electroactive surface areas (A) of an ordinary gold nanoparticle (AuNP) modified electrode and the PAMAM–rGO modified electrode, which was determined according to the Randles–Sevcik equation:[39] $I_p = 2.69 \times 10^5 AD^{1/2}n^{3/2}\upsilon^{1/2}c$. As shown in Fig. 4A and B, the peak currents (I_p) of both AuNP and PAMAM–rGO modified electrodes were proportional to the square root of scan rate. Based on this method, with the constant parameters of D, c and n, we could successfully acquire an approximate value of A. Electroactive surface areas of 16.48 mm^2 and 25.75 mm^2 for the AuNP and PAMAM–rGO modified electrodes were obtained, respectively. The electroactive surface area of the PAMAM–rGO modified electrode increased by about 56.3% compared with the AuNP modified electrode, which provided effective evidence for the superior conductivity of the PAMAM–rGO film as expected.

Optimization of assay conditions

It was well known that the performance of the electrochemical enzyme-catalyzed analysis was related to the concentration of H_2O_2 in the measuring system. Therefore, before testing the thrombin, we first studied the effect of H_2O_2 concentration. The assay was carried out by using the aptasensor toward the catalytic reduction of H_2O_2 after incubation with 1 nM thrombin. As can be seen from Fig. 5A, the peak current increased with the increase of H_2O_2 concentration, and reached plateau regions at

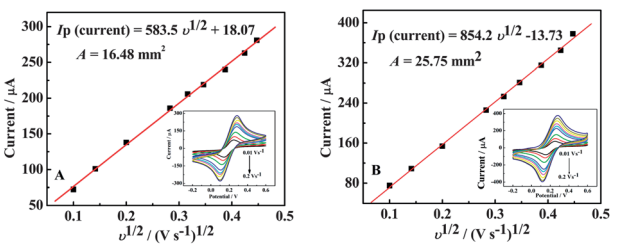

Fig. 4 CVs of AuNP (A) and PAMAM–rGO (B) modified GCEs in 5.0 mM $Fe(CN)_6^{4-/3-}$ at different scan rates from 10 to 200 mV s^{-1}. Insets show the linear relations of the AuNP and PAMAM–rGO modified GCEs with the anodic peak current against the square root of scan rate.

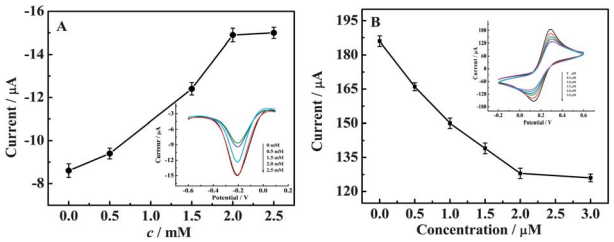

Fig. 5 (A) The influence of the concentration of H_2O_2 on the current response of the aptasensor. The inset shows the dependence of the DPV response on each concentration. (B) The optimization of TBA concentration. The inset shows the different peak currents for each concentration of TBA.

a concentration of 2.0 mM. Thus, the H_2O_2 concentration chosen was 2 mM.

To acquire an optimal electrochemical response, the concentration of primary TBA should be optimized. 20 μL of TBA of different concentrations was attached onto the modified electrode and investigated in 5.0 mM $Fe(CN)_6^{4-/3-}$. As shown in Fig. 5B, the response current values decreased with the increase of the primary TBA concentration, and the current tended to level off when the concentration of TBA was higher than 2 μM. Therefore, 2 μM of TBA was used for the detection of thrombin in the following experiments.

Detection of thrombin based on DPV

Under the optimal assay conditions, the quantitative analysis of the present biosensor was evaluated by detecting thrombin in standard solutions using the DPV technique and adding 2.0 mM H_2O_2 into an electrolytic cell using the developed sandwich-type assay with $mSiO_2$@MWCNT–Thi–PtNP–hemin/G-quadruplex bioconjugate as a tracer label. As a result, the DPV signal responses increased with the increment of thrombin concentrations after the complementary pairing interaction (Fig. 6A). The dose response curve of the proposed aptasensor for thrombin showed a good linear relationship between the reduction peak currents and the analyte concentrations. The linear range covered was from 0.0001 to 80 nM with a regression equation of the form I (μA) = $-1.804c$ − 14.98 and a linear correlation coefficient of 0.9949 (Fig. 6B). A detection limit of 50 fM was determined according to a signal-to-noise ratio of 3.

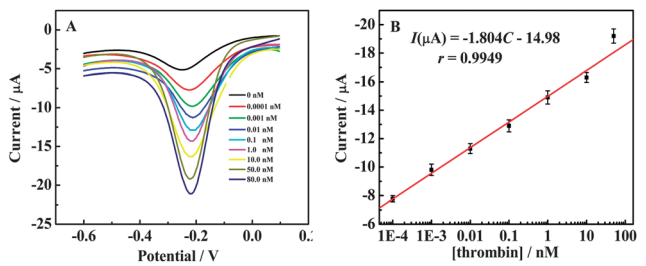

Fig. 6 (A) DPV curves of the resulting aptasensor for thrombin detection at different concentrations in 0.1 M PBS (pH 7.0) containing 2.0 mM H_2O_2. (B) The calibration curve of electrocatalytic current response *versus* thrombin at various concentrations.

The higher sensitivity and wider linear range of the developed aptasensor investigated in PBS (pH 7.0) containing 2.0 mM H_2O_2 should be ascribed to the significant amplification of the $mSiO_2$@MWCNT–Thi–PtNP nano-hybrid film and the pseudo-bienzymatic activity of the hemin/G-quadruplex which acted as a HRP-mimicking DNAzyme. In addition, the analytical performance of the developed aptasensor for thrombin detection has been compared with those of other similar sandwiched aptasensors reported in the literature. The results are summarized in Table S1 (see ESI†).

Selectivity, reproducibility and stability of the aptasensor

To evaluate the specificity of the electrochemical aptasensor, we challenged the system with other possible interferences, and the results are exhibited in Fig. 7. With some amount of nontarget molecules, such as bovine serum albumin (BSA), hemoglobin (Hb) and platelet-derived growth factor (PDGF), no apparent change in the current was observed compared with that of the blank test. However, the presence of target thrombin resulted in a dramatic increase in the current. Even when BSA, Hb and PDGF coexisted with thrombin, the electrochemical response was almost the same as that of thrombin, indicating the high specificity of the proposed aptasensor for thrombin detection.

The reproducibility of the aptasensor played a critical role in analyzing biological samples *in situ* without separation. Therefore, the reproducibility of the aptasensor was evaluated by using the variation coefficient of the intra-assays and inter-assays. Analyzed from experimental results, the relative standard deviation of the intra-assay was 4.8% at 1 nM thrombin, whereas the relative standard deviation of the inter-assay with various batches was 6.2% at 1 nM thrombin. Thus, the reproducibility and precision of the aptasensor were acceptable. In addition, the aptasensor decreased gradually and retained 94.4% of its initial current after 5 days of storage and 90% after 20 days of storage, suggesting the acceptable stability of the proposed aptasensor.

Analytical application of the aptasensor

Thrombin exists in the form of thrombinogen in healthy human serum samples. To further investigate the analytical reliability and possible application of the proposed aptasensor, recovery

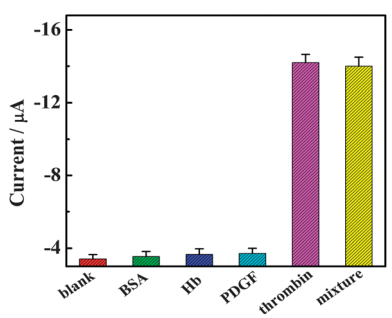

Fig. 7 Study of the possible interferences tested with the proposed assay: BSA (10 nM), Hb (10 nM), PDGF (10 nM) and their mixture with thrombin.

Table 1 Determination of thrombin added in human blood serum ($n = 5$) with the proposed aptasensor

Sample	Added thrombin/nM	Found thrombin/nM	Recovery/%	RSD (%)
1	0.0100	0.01071	107.1	4.7
2	0.1000	0.09110	91.10	3.7
3	5.000	5.038	100.1	5.6
4	10.00	9.984	99.84	6.7
5	30.00	30.17	100.5	7.8

experiments were performed by standard addition methods in human serum. During this process, a series of samples were prepared by adding thrombin of different concentrations into 10-fold-diluted healthy human serum samples to examine the feasibility of the proposed strategy. As shown in Table 1, the recovery (between 91.10% and 107.1%) and the relative standard deviation values (between 3.7% and 7.8%) were acceptable. These results indicated that the proposed electrochemical aptasensor provided a potential application in real biological samples.

Conclusions

In summary, this work has designed a new paradigm electrochemical aptasensor for the sensitive detection of thrombin based on integrating hemin/G-quadruplex with functionalized PtNP–Thi–mSiO_2@MWCNT nanocomposites both as a trace label and for signal enhancement. Firstly, the mSiO_2@MWCNT nanocomposites with a high aspect ratio could increase the amount of electron mediator Thi, PtNPs and hemin/G-quadruplex bioelectrocatalytic complex, and also had good biocompatibility and a suitable microenvironment for stabilizing the aptamer assembly. Moreover, PtNPs and hemin/G-quadruplex as electrocatalysts could further amplify the response signals of Thi and improve the sensitivity in the presence of H_2O_2 in an electrolytic cell. Secondly, the PAMAM–rGO nano-hybrid film not only provided a large accessible surface area to capture a large number of primary aptamers but also facilitated electron transfer from Thi to the electrode, thus amplifying the detection response. In view of these advantages, we anticipate that this strategy may offer a new approach to construct an electrochemical amplification assay with high sensitivity and selectivity for successful application in clinical diagnosis.

Acknowledgements

This work was financially supported by the NNSF of China (21275119, 21075100), State Key Laboratory of Electroanalytical Chemistry (SKLEAC2010009), Specialized Research Fund for the Doctoral Program of Higher Education (20100182110015), the Fundamental Research Funds for the Central Universities (XDJK2012A004, XDJK2013A008), Ministry of Education of China (Project 708073) and the Postgraduate Science and Technology Innovation Program of Southwest China University (Grant no. KB2010006).

Notes and references

1 J. Wu, Z. F. Fu, F. Yan and H. X. Ju, *TrAC, Trends Anal. Chem.*, 2007, **26**, 679.
2 S. I. Stoeva, J. S. Lee, J. E. Smith, S. T. Rosen and C. A. Mirkin, *J. Am. Chem. Soc.*, 2006, **128**, 8387.
3 J. J. Storhoff, S. S. Marla, P. Bao, S. Hagenow, H. Mehta, A. Lucas, V. Garimella, T. Patno, W. Buckingham, W. Cork and U. R. Muller, *Biosens. Bioelectron.*, 2004, **19**, 875.
4 Y. Jiang, X. Fang and C. Bai, *Anal. Chem.*, 2004, **76**, 5230.
5 S. Guo and E. Wang, *Nano Today*, 2011, **6**, 240.
6 S. Zhang, H. Zhong and C. Ding, *Anal. Chem.*, 2008, **80**, 7206.
7 Y. Du, B. Li, H. Wei, Y. Wang and E. Wang, *Anal. Chem.*, 2008, **80**, 5110.
8 M. Liss, B. Petersen, H. Wolf and E. Prohaska, *Anal. Chem.*, 2002, **74**, 4488.
9 M. Minunni, S. Tombelli, J. Fonti, M. M. Spiriti, M. Mascini, P. Bogani and M. Buiatti, *J. Am. Chem. Soc.*, 2005, **127**, 7966.
10 S. J. Guo, Y. Du, X. Yang, S. J. Dong and E. Wang, *Anal. Chem.*, 2011, **83**, 8035.
11 S. Niyogi, E. Bekyarova, M. E. Itkis, J. L. Mcwilliams, M. A. Hamon and R. C. Haddon, *J. Am. Chem. Soc.*, 2006, **128**, 7720.
12 X. R. Zhang, B. P. Qi, Y. Li and S. S. Zhang, *Biosens. Bioelectron.*, 2009, **25**, 259.
13 H. X. Wang, Y. Liu, C. C. Liu, J. Y. Huang, P. Y. Yang and B. H. Liu, *Electrochem. Commun.*, 2010, **12**, 258.
14 Y. Du, C. Chen, M. Zhou, S. Dong and E. Wang, *Anal. Chem.*, 2011, **83**, 1523.
15 S. Guo and E. Wang, *Anal. Chim. Acta*, 2007, **598**, 181.
16 L. Wang, C. Zhu, L. Han, L. Jin, M. Zhou and S. Dong, *Chem. Commun.*, 2011, **47**, 7794.
17 Y. C. Xing, *J. Phys. Chem. B*, 2004, **108**, 19255.
18 Z. L. Liu, X. H. Lin, J. Y. Lee, W. D. Zhang, M. Han and L. M. Gan, *Langmuir*, 2002, **18**, 4054.
19 W. Z. Li, C. H. Liang, W. J. Zhou, J. S. Qiu, Z. H. Zhou and G. Q. Sun, *J. Phys. Chem. B*, 2003, **107**, 6292.
20 G. G. Wildgoose, C. E. Banks and R. G. Compton, *Small*, 2006, **2**, 182.
21 J. L. Hudson, M. J. Casavant and J. M. Tour, *J. Am. Chem. Soc.*, 2004, **126**, 11158.
22 J. J. Stephenson, J. L. Hudson, S. Azad and J. M. Tour, *Chem. Mater.*, 2006, **18**, 374.
23 S. D. Yang, X. G. Zhang, H. Y. Mi and X. G. Ye, *J. Power Sources*, 2008, **175**, 26.
24 M. Kanungo, H. S. Isaacs and S. S. Wong, *J. Phys. Chem. C*, 2007, **111**, 17730.
25 K. L. Ding, B. J. Hu, Y. Xie, G. An, R. Tao, H. Y. Zhang and Z. M. Liu, *J. Mater. Chem.*, 2009, **19**, 3725.
26 Y. L. Yuan, G. P. Liu, R. Yuan, Y. Q. Chai, X. X. Gan and L. J. Bai, *Biosens. Bioelectron.*, 2013, **42**, 474.
27 S. Bi, S. Y. Hao, L. Li and S. S. Zhang, *Chem. Commun.*, 2010, **46**, 6093.
28 J. Liu, Z. Cao and Y. Lu, *Chem. Rev.*, 2009, **109**, 1948.
29 D. S. Wilson and J. W. Szostak, *Annu. Rev. Biochem.*, 1999, **68**, 611.
30 R. R. Breaker and G. F. Joyce, *Chem. Biol.*, 1994, **1**, 223.

31 P. Travascio, Y. F. Li and D. Sen, *Chem. Biol.*, 1998, **5**, 505.
32 B. Shlyahovsky, D. Li, E. Katz and I. Willner, *Biosens. Bioelectron.*, 2007, **22**, 2570.
33 Y. Xiao, V. Pavlov, T. Niazov, A. Dishon, M. Kotler and I. Willner, *J. Am. Chem. Soc.*, 2004, **126**, 7430.
34 D. Li, B. Shlyahovsky, J. Elbaz and I. Willner, *J. Am. Chem. Soc.*, 2007, **129**, 5804.
35 G. Pelossof, R. T. Vered, J. Elbaz and I. Willner, *Anal. Chem.*, 2010, **82**, 4396.
36 P. Y. Ge, W. Zhao, Y. Du, J. J. Xu and H. Y. Chen, *Biosens. Bioelectron.*, 2009, **24**, 2002.
37 T. Y. You, O. Niwa, M. Tomita and S. Hirono, *Anal. Chem.*, 2003, **75**, 2080.
38 R. Polsky, R. Gill, L. Kaganovsky and I. Willner, *Anal. Chem.*, 2006, **78**, 2268.
39 A. J. Bard and L. R. Faulkner, *Electrochemical methods: fundamentals and applications*, Wiley, 2nd edn, New York, 1980.